

## **INITIAL CHARACTERIZATION OF V-4Cr-4Ti AND MHD COATINGS EXPOSED TO FLOWING Li – ORNL Loop Team: B. A. Pint, S. J. Pawel, M. Howell, J. L. Moser, G. W. Garner, M. L. Santella, P. F. Tortorelli, F. W. Wiffen and J. R. Distefano (Oak Ridge National Laboratory)**

### **OBJECTIVE**

Conduct an experiment with flowing Li in a thermal gradient to determine the compatibility of V-4Cr-4Ti and a multi-layer electrically-insulating coating needed to reduce the magneto hydrodynamic (MHD) force in the first wall of a lithium cooled blanket.

### **SUMMARY**

A mono-metallic V-4Cr-4Ti thermal convection loop was operated in vacuum ( $\sim 10^{-5}$ Pa) at a maximum Li temperature of 700°C for 2,355h and Li flow rate of 2-3 cm/s. Two-layer, physical vapor deposited  $Y_2O_3$ -vanadium, electrically-insulating coatings on V-4Cr-4Ti substrates as well as uncoated tensile and sheet specimens were located in the flow path in the hot and cold legs. After exposure, specimens at the top of the hot leg showed a maximum mass loss equivalent to  $\sim 1.3\mu\text{m}$  of uniform metal loss. Elsewhere, small mass gains were observed on the majority of specimens that also showed an increase in hardness and room temperature yield stress and a decrease in ductility consistent with interstitial uptake. Specimens that lost mass showed a decrease in yield stress and hardness. Profilometry showed no significant thickness loss from the coatings.

### **PROGRESS AND STATUS**

#### **Introduction**

One of the critical unresolved issues for the vanadium-lithium blanket concept[1,2] (and any liquid metal concept) in a deuterium/tritium fueled fusion reactor[3,4] is the need to reduce the pressure drop associated with the magnetohydrodynamic (MHD) effect of a conducting liquid flowing across the magnetic field lines. One solution to the MHD problem is to decouple the structural wall from the liquid metal with an electrically insulating coating or flow channel insert (FCI).[5] This coating application requires a thin, crack-free,[6] durable layer with a relatively high electrical resistance.[7] While a “self-healing” layer is possible in corrosion where a re-passivation can occur with the re-formation of a surface oxide, this concept is not applicable to functional (i.e. electrically resistant) coatings because a defect that shorts the coating is unlikely to “heal”. Therefore, a robust coating system or a FCI is needed for this application. Due to incompatibility between Li and virtually all candidate insulating oxides,[8-12] the current focus of the U.S. MHD coating program[10-12] is on evaluating the compatibility of durable, multi-layer coatings[7,13] where a vanadium overlayer prevents direct contact between the insulating oxide layer and Li. This concept shifts the compatibility concern from the oxide layer to the thin vanadium overlayer. In order to verify that a thin,  $\sim 10\mu\text{m}$ , V layer is sufficiently compatible with Li to function in a long-term situation, a mono-metallic thermal convection loop was designed and built to expose thin V overlayers to flowing Li. The loop was operated with a peak temperature of  $\sim 700^\circ\text{C}$  for 2,355h.[14] Initial characterization of the coatings and V-4Cr-4Ti specimens in the loop are presented. Additional characterization of the coatings will be presented in future publications.

#### **Experimental Procedure**

A harp-shaped thermal convection loop was constructed of drawn tubing made from the large U.S. heat of V-3.8wt.%Cr-3.9%Ti (Heat#832665 made at Wah Chang, Albany, OR)[15] with an outer diameter of 19mm and a 1.6mm wall thickness. Additional details of the loop construction and operation were reported previously.[14,16] The experiment was conducted in a stainless steel vacuum chamber. Wire and

specimens, all made from the same V-4Cr-4Ti heat, formed ~80cm long chains that were placed in the hot and cold legs. The 29 specimens in each chain consisted of alternating interlocked tabs (31 x 13 x 0.9mm), which held the chain in the center of the tube, and pairs of miniature tensile specimens (type SS-3: 25 x 4 x 0.9mm). Prior to exposure, the tensile specimens were vacuum annealed for 1h at 1050°C. Specimen mass was measured on a microbalance with a  $\pm 0.01$  mg/cm<sup>2</sup> error. Six of the exposed tabs had an electron-beam physical vapor deposited (EB-PVD) Y<sub>2</sub>O<sub>3</sub> coating completely covered by an outer layer of unalloyed vanadium on one side.[11,12] The coatings were made in two batches[17] and the unexposed coating thicknesses are shown later in Table 2.

Sticks of Li (as-received batch: <100ppmw N, 95ppmw C and 950ppmw O)[12] totalling ~275g were loaded into the fill tank in a glove box and the tank lid was welded shut. The Li in the tank was melted to begin the experiment. A much larger than expected temperature gradient was observed during the first 1248h phase of operation. Initially, the difference between the top and bottom of the hot leg was 340°C and slowly increased to almost 400°C, Figure 1. Using thermocouples to measure the movement of a hot spot created by a pair of SiC heating elements, the Li velocity was estimated to be ~2 cm/s during the first phase. After an unexplained upset that occurred between 1248-1262h, Figure 1, the cold leg temperatures increased and the gradient was only ~225°C suggesting a faster Li velocity of >3cm/s (based on the lower T gradient) which was similar to the velocity measured in the stainless steel test loop operated at ~550°C.[16] However, the higher cold leg temperatures prevented an accurate velocity measurement. The inability to maintain the peak temperature at 700°C for the second operational phase (Fig. 1) was subsequently attributed to a loose furnace connection. One hypothesis for the high first phase T is that the Li flow was restricted by the specimen chain and that specimen movement or the chain breaking (which was *not* observed during disassembly) allowed more rapid Li flow during the second phase.

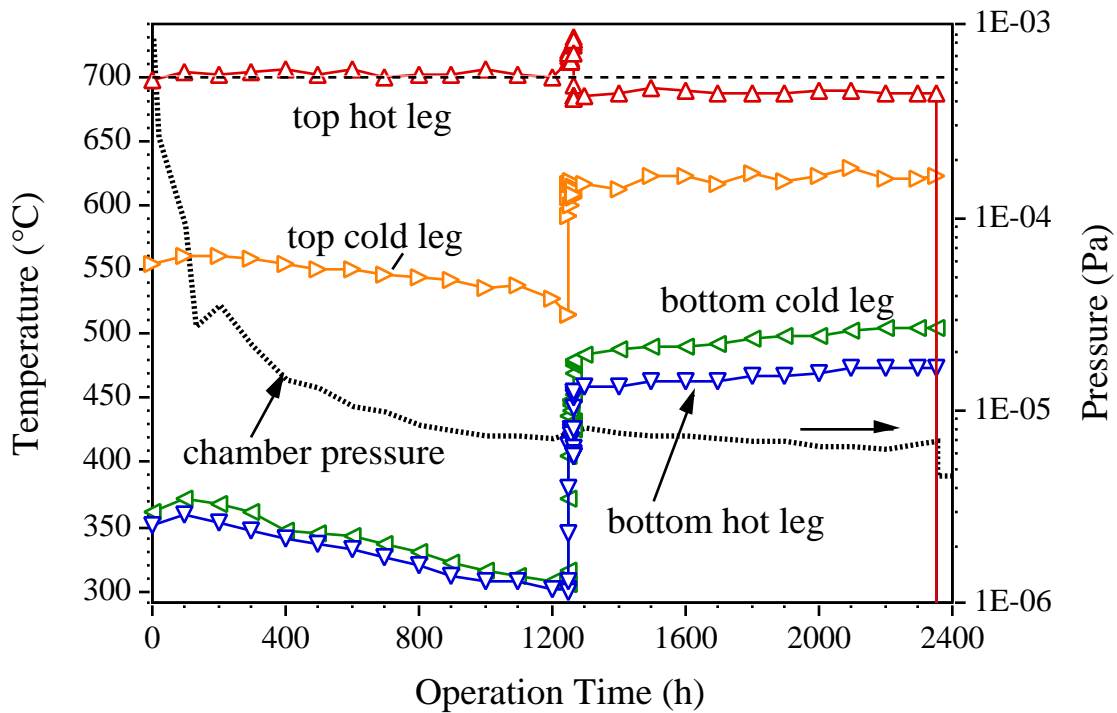


Figure 1. Temperatures in loop thermal wells and chamber pressure as a function of operation time for the V-4Cr-4Ti loop experiment.

After the experiment ended, the chamber was opened and the loop inverted and re-instrumented. The chamber was then pumped down and the loop was heated to  $\sim 400^\circ\text{C}$  allowing the Li to drain back into the tank. The loop was then cut open in an Ar-filled glove box. The top tab specimens were not found to be located below the cross-over joints in the hot and cold leg as intended and therefore could have restricted Li flow. The specimen chains were removed from the tubing and residual Li was removed using liquid ammonia followed by soaking in ethanol and then water.

Initial characterization of the specimens and tubing included metallographic cross-sections, hardness (Vickers, 300g) measurements, chemical analysis using combustion and inductively coupled plasma analysis, and room temperature tensile testing at  $10^{-3}\text{s}^{-1}$  strain rate. Selected specimens were examined using scanning electron microscopy (SEM) equipped with energy dispersive x-ray (EDX) analysis. The EB-PVD coatings were examined by SEM/EDX, contact profilometry and x-ray diffraction (XRD).

## Results and Discussion

Figure 2 shows the mass change data for both specimen chains with the nominal temperature profiles in the hot and cold legs. Mass losses in seven specimens from the hot leg were consistent with dissolution of metal (maximum  $\sim 0.6\text{mg}/\text{cm}^2$  is equivalent to  $1\mu\text{m}$  vanadium) and/or loss of interstitials such as oxygen. Assuming linear kinetics, the maximum observed loss is the equivalent to  $\sim 2.5\text{mg}/\text{m}^2\text{h}$  which is similar to the rate reported previously at  $538^\circ\text{C}$  for V-15Cr-5Ti with Li+50ppm N in a pumped loop (1 l/min).[18] However, the results in that study were complicated by the use of a stainless steel loop. Prior results in a mono-metallic loop at  $700^\circ\text{C}$  reported small mass gains after 1,000h.[19]

The three specimens at the very top of the hot leg did not show a mass loss, Figure 2, which may be explained by temperature or Li flow differences. As mentioned previously, the chain was not positioned in

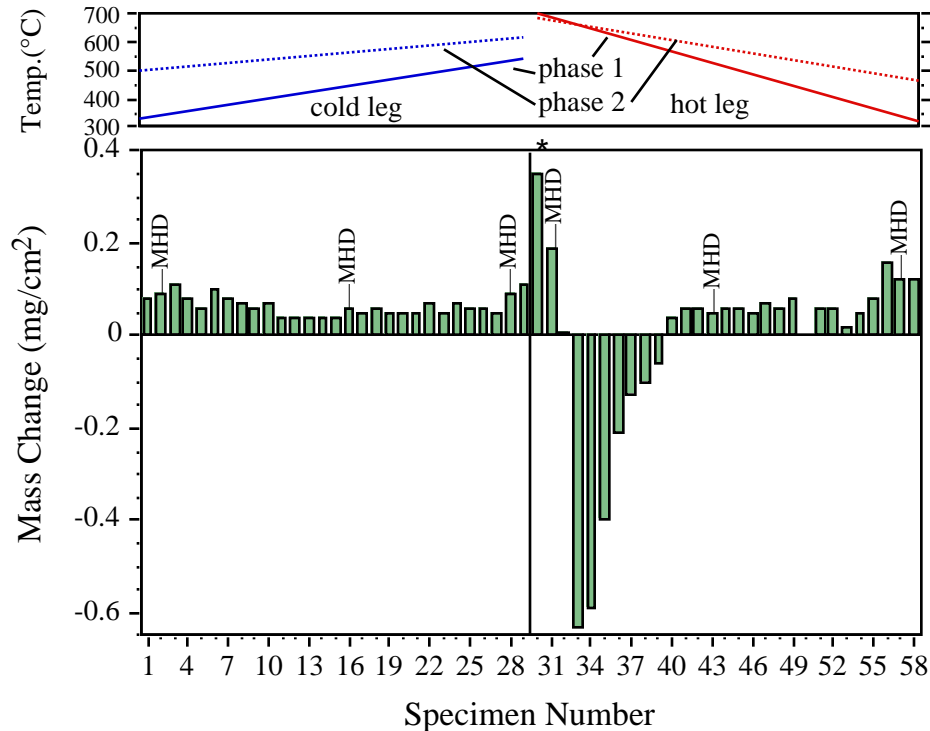


Figure 2. Specimen mass change for V-4Cr-4Ti specimens in the hot and cold leg of the mono-metallic loop along with the nominal temperature that the specimens saw during the two phases of operation. In the hottest section of the loop, mass losses were observed, elsewhere, small mass gains were measured.

the loop as intended and the first specimen in the chain (\* in Figure 2) appeared to be above the Li flow path which may explain its high mass gain (i.e. higher interstitial pickup and/or less metal transfer). The second and third specimens appeared to be within the Li flow path although they were located above the hot leg furnace ~2cm from the hot leg thermal well where the 700°C temperature was measured. Elsewhere in both legs, all of the specimens showed a small mass gain. The location of the six EB-PVD coated specimens also are shown in Figure 2, and each had a mass gain comparable to neighboring specimens.

Chemical analyses of the interstitial contents for selected tab specimens at the top, bottom and middle of the hot and cold leg are shown in Figure 3. As expected, there was a decrease in the O content for all of the specimens and an increase in the N and C content. However, that effect was particularly strong in the hottest section where the O content decreased to 20ppmw and the N content increased to 1590ppmw. There was no significant change in the V, Cr or Ti contents measured. Table 1 shows the changes in interstitial content for each of the measured locations and the measured and calculated mass change based on the chemistry change. The small mass change observed in most of the specimens is likely associated with the uptake of N and C minus the decrease in O. However, the mass gains in the coldest parts of the loop are not explained by this uptake and may be due to a small amount of metal deposition, e.g., a 0.06mg/cm<sup>2</sup> mass gain would be equivalent to a ~100nm layer of metal. For the highest temperature specimen analyzed from the hot leg, the large increase in N content resulted in a calculated net mass gain, suggesting that the metal loss may have been on the order of 0.8mg/cm<sup>2</sup> or ~1.3µm.

Figure 4 shows results from room temperature tensile tests of specimens from the hot and cold legs as well as average values for three unexposed specimens from the same specimen batch which have similar properties as those measured in prior studies.[20-22] The 0.2% yield and ultimate tensile strengths increased in specimens as the exposure temperature decreased, Figure 4a. The mass gain and

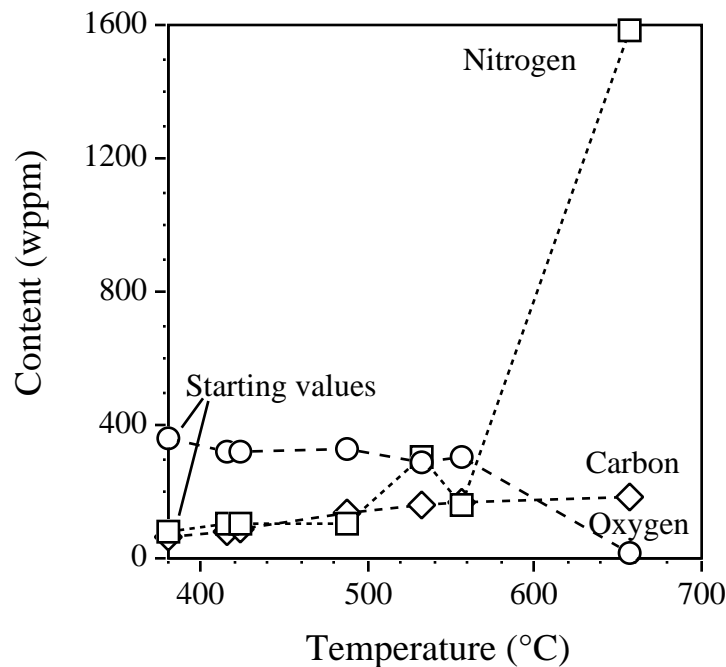


Figure 3. Measured O, C and N values for specimens at six locations in the loop. A slight drop in O and increase in C and N was observed except for the hottest location where there was a large increase in N and a decrease in O to 20ppmw.

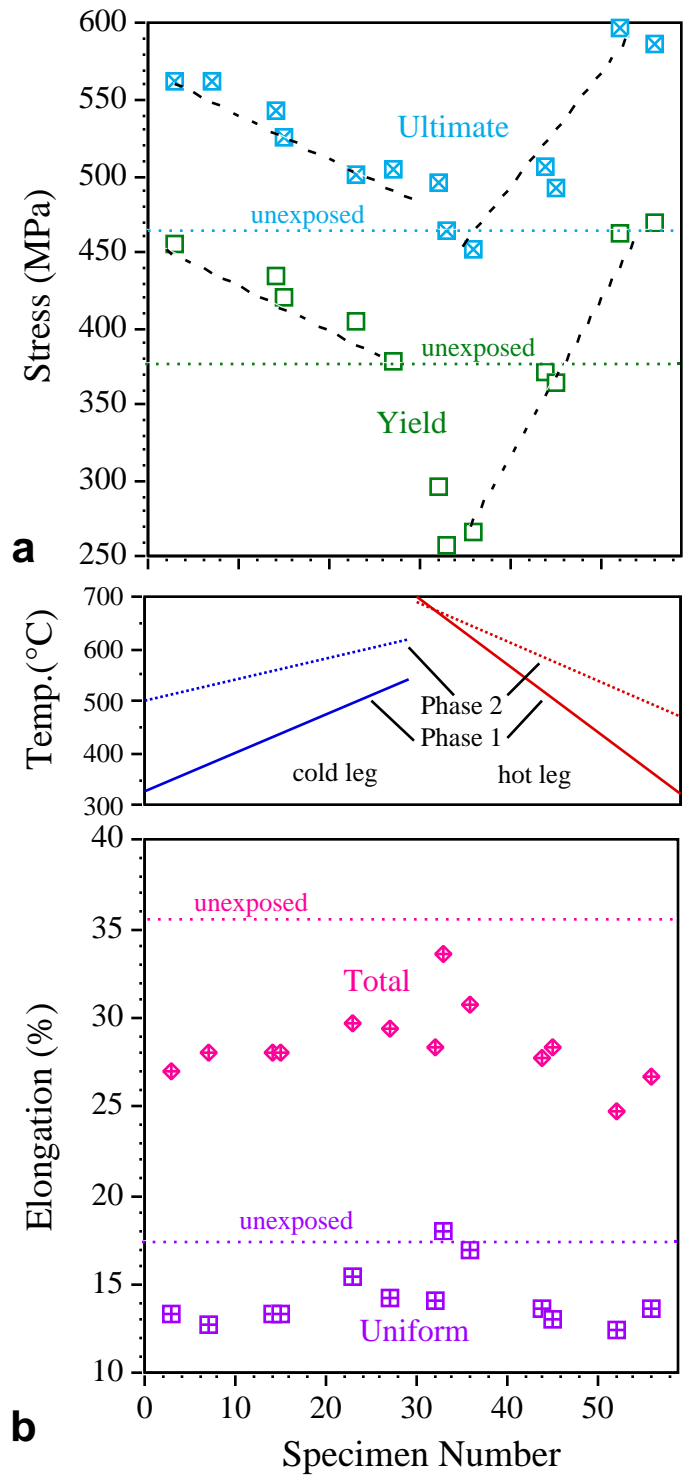


Figure 4. Room temperature tensile properties of a subset of V-4Cr-4Ti specimens after exposure in a mono-metallic loop: (a) 0.2% yield and ultimate tensile stress and (b) uniform and total elongation. The specimen in the hottest locations that lost mass showed a decrease in strength and less loss in ductility than the other specimens that had a mass gain after exposure.

Table 1. Measured interstitial composition and mass gain data and calculated mass gain based on the interstitial composition change. The measured mass change is the average of the two tab specimens that were chemically analyzed.

Location	Temperature	Measured Change (wppm)			Mass Change (mg/cm <sup>2</sup> )	
		O	N	C	Measured	Calculated
Top Hot Leg	657	-340	+1510	+120	-0.50	+0.30
Top Cold Leg	556	-50	+80	+100	+0.06	+0.03
Middle Hot Leg	532	-70	+230	+90	+0.06	+0.06
Middle Cold Leg	487	-30	+30	+70	+0.04	+0.02
Bottom Cold Leg	423	-40	+30	+20	+0.09	+0.002
Bottom Hot Leg	416	-40	+30	+10	+0.12	0.0
Starting content		360	80	70		

associated N and C increase for many of these specimens suggests interstitial hardening as a mechanism to increase the yield and ultimate tensile stresses. The variation with temperature is likely due to thermal ageing during the 2,355 h exposure. The specimens from the hot leg with mass losses showed a large decrease in yield strength, which is not consistent with the large N increase but is consistent with the large drop in O content, Table 1. In Figure 4b, modest decreases in the uniform and total elongations also were observed compared to unexposed specimens. These ductility values are somewhat higher than were previously reported.[19] Additional tensile specimens will be tested at 500°C to compare to prior work on Li-exposed material.[23]

Figure 5 shows the change in average hardness (from a starting value of 204±6 Hv for the starting unannealed cold-rolled material) and mass for tab specimens as a function of nominal average temperature based on their location in the specimen chain and assuming a linear temperature change between the thermal wells on the hot and cold legs. The hardness, but not the net mass change, showed a correlation with exposure temperature. Hardness values and standard deviations are based on 7 measurements across the polished ~0.9mm tab cross-section. The decrease in hardness with temperature is consistent with thermal annealing of the original cold-rolled microstructure. Figure 6 shows etched metallographic cross-sections of the hot leg tab specimens from Figure 5 and Table 1 with the surface at the top of each figure. The as-rolled microstructure is shown in Figure 5a. There was little change in the microstructure at the bottom of the hot leg at the lowest temperature, Figure 5b. The specimen exposed at ~655°C (Fig. 5d) showed a much larger re-crystallized grain size and a surface layer which appeared to be depleted in precipitates. A similar layer or recrystallization was not observed in any of the other specimens from the cold leg. The near-surface microhardness has not been investigated yet. Prior work,[18] showed a ~30µm deep microhardness gradient in V-15Cr-5Ti after exposure at 482-538°C.

Finally, Table 2 shows the profilometry data for the EB-PVD coated specimens after exposure. Batch 1 coatings were exposed at the higher temperatures because they were of higher initial quality.[17] No significant loss in thickness was detected. However, the unexposed coated specimens were concave indicating that the as-deposited coatings were under compression while the coated specimens exposed at the highest temperatures were all convex after exposure which could indicate stress relief or some type of degradation such as cracking or expansion due to reaction with Li. The EB-PVD Y<sub>2</sub>O<sub>3</sub>/V coatings showed no significant loss in thickness, however, further characterization is needed to determine their electrical resistance and microstructure after exposure. In order to measure the electrical resistance, a procedure needs to be developed to electrically isolate the oxide coating from the vanadium overlayer. After the resistance measurement, the coatings will be sectioned to evaluate the microstructure.

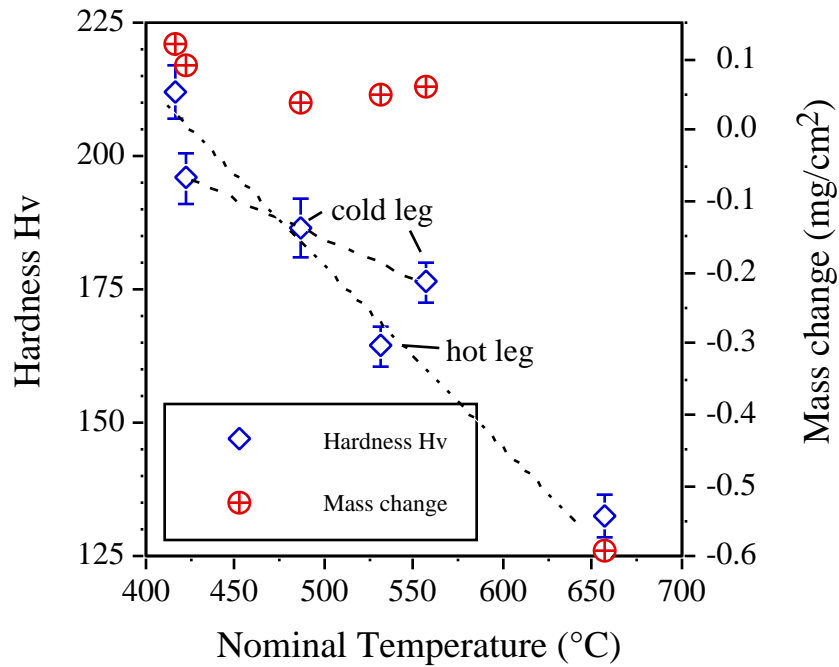


Figure 5. Average hardness measurements as a function of nominal exposure temperature along the hot and cold legs of the mono-metallic loop. The hardness decreased with exposure temperature in both legs.

Currently, a 700°C 2,350h anneal is being conducted on several tensile specimens, a tab specimen and an unexposed MHD coating. The specimens were placed in a quartz ampoule and evacuated to limit reaction during the anneal. These specimens will provide a baseline for changes in the microstructure and

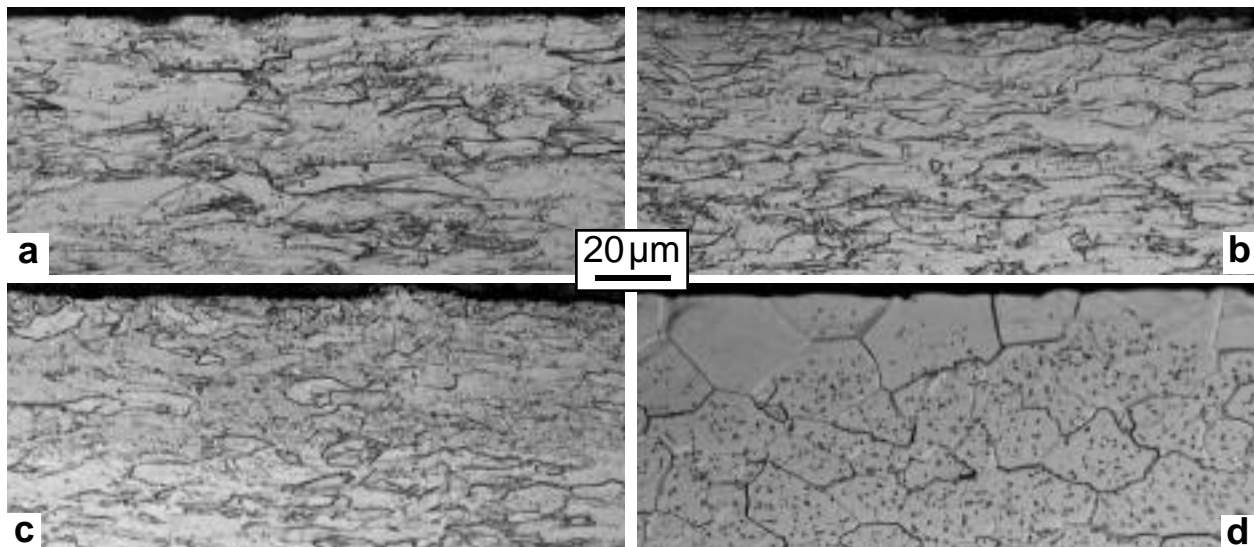


Figure 6. Light microscopy of unannealed V-4Cr-4Ti tab specimens (a) unexposed and after exposure to flowing Li (b) bottom of the hot leg (~415°C), (c) middle of the hot leg (~530°C) and (d) top of the hot leg (~655°C) where the surface grains appear depleted in precipitates.

Table 2. Profilometry data of the  $V/Y_2O_3$  coatings on V-4Cr-4Ti substrates after exposure to flowing Li for 2,355h in a V-4Cr-4Ti loop with a maximum temperature of 700°C.

Location	Batch 1		Batch 2	
	V layer	$Y_2O_3$ layer	V layer	$Y_2O_3$ layer
Unexposed	9 $\mu$ m	13 $\mu$ m	10 $\mu$ m	17 $\mu$ m
Top Hot Leg	8	12		
Top Cold Leg	8	11		
Middle Cold Leg	7	12		
Bottom Cold Leg			10	15
Bottom Hot Leg			9	17
Middle Hot Leg			9	16
As-deposited*	7.4 $\pm$ 0.3	11.7 $\pm$ 0.5	9.9 $\pm$ 0.4	15.7 $\pm$ 0.9

\* Reference 17

properties due to the temperature exposure without the effect of flowing Li.

## References

- [1] R. J. Kurtz, K. Abe, V. M. Chernov, D. T. Hoelzer, H. Matsui, T. Muroga and G. R. Odette, J. Nucl. Mater. 329-333 (2004) 47.
- [2] T. Muroga, J. M. Chen, V. M. Chernov, K. Fukumoto, D. T. Hoelzer, R. J. Kurtz, T. Nagasaka, B. A. Pint, M. Satou, A. Suzuki and H. Watanabe, J. Nucl. Mater. 367-370 (2007) 780.
- [3]. I. R. Kirillov, C. B. Reed, L. Barleon and K. Miyazaki, Fus. Eng. Design 27 (1995) 553.
- [4] L. Barleon, V. Casal and L. Lenhart, Fus. Eng. Design 14 (1991) 401.
- [5] S. Malang, H. U. Borgstedt E. H. Farnum, K. Natesan and I. V. Vitkovski, Fus. Eng. Design 27 (1995) 570.
- [6] L. Bühler, Fus. Eng. Design, 27 (1995) 650.
- [7] Y. Y. Liu and D. L. Smith, J. Nucl. Mat. 141-143 (1986) 38.
- [8] J. E. Battles, Intern. Mater. Rev. 34 (1989) 1.
- [9] T. Terai, et al., J. Nucl. Mater. 233-237 (1996) 1421.
- [10] B. A. Pint, P. F. Tortorelli, A. Jankowski, J. Hayes, T. Muroga, A. Suzuki, O. I. Yeliseyeva and V. M. Chernov, J. Nucl. Mater. 329-333 (2004) 119.
- [11] B. A. Pint J. L. Moser and P. F. Tortorelli, Fus. Eng. Des. 81 (2006) 901.
- [12] B. A. Pint, J. L. Moser, A. Jankowski and J. Hayes, J. Nucl. Mater. 367-370 (2007) 1165.
- [13] I. V. Vitkovsky, et al., Fus. Eng. Design, 61-62 (2002) 739.
- [14] B. A. Pint, S. J. Pawel, M. Howell, J. L. Moser, G. Garner, M. Santella, P. F. Tortorelli and J. R. Distefano, DOE/ER-0313/42 (2007) 2.
- [15] D. L. Smith, H. M. Chung, B. A. Loomis and H.-C. Tsai, J. Nucl. Mater. 233-237 (1996) 356.
- [16] B. A. Pint, et al., DOE-ER-0313/41 (2006) 2.
- [17] A. F. Jankowski and B. A. Pint, [unpublished research](#) (2007).
- [18] O. K. Chopra and D. L. Smith, J. Nucl. Mater. 155-157 (1988) 683.
- [19] V. A. Evtikhin, I. E. Lyublinski and A. V. Vertkov, J. Nucl. Mater. 258-263 (1998) 1487.
- [20] H. M. Chung, B. A. Loomis and D. L. Smith, Fus. Eng. Des. 29 (1995) 455.
- [21] K. Fukumoto, T. Morimura, T. Tanaka, A. Kimura, K. Abe, H. Takahashi and H. Matsui, J. Nucl. Mater. 239 (1996) 170.
- [22] B. A. Pint and J. R. DiStefano, Oxid. Met. 63 (2005) 33.
- [23] T. Nagasaka, T. Muroga, M. M. Li, D. T. Hoelzer, S. J. Zinkle, M. L. Grossbeck and H. Matsui, Fus. Eng. Des. 81 (2006) 307-313.